

# A Keck/DEIMOS Spectroscopy of Ly $\alpha$ Blobs at Redshift $z = 3.1$ <sup>1,2</sup>

Yuichi Matsuda <sup>3</sup>, Toru Yamada <sup>4</sup>, Tomoki Hayashino <sup>5</sup>, Ryosuke Yamauchi <sup>5</sup>, Yuki Nakamura <sup>5</sup>

matsdayi@kusastro.kyoto-u.ac.jp

## ABSTRACT

We present the results of an intermediate resolution ( $\sim 2 \text{ \AA}$ ) spectroscopy of a sample of 37 candidate Ly $\alpha$  blobs and emitters at redshift  $z = 3.1$  using the DEIMOS spectrograph on the 10 m Keck telescope. The emission lines are detected for all the 37 objects and have variety in their line profiles. The Ly $\alpha$  velocity widths (FWHM) of the 28 objects with higher quality spectra, measured by fitting a single Gaussian profile, are in the range of  $150 - 1700 \text{ km s}^{-1}$  and correlate with the Ly $\alpha$  spatial extents. All the 12 Ly $\alpha$  blobs ( $\geq 16 \text{ arcsec}^2$ ) have large velocity widths of  $\gtrsim 500 \text{ km s}^{-1}$ . While there are several possible physical interpretations of the Ly $\alpha$  velocity widths (motion of gravitationally-bound gas clouds, inflows, merging of clumps, or outflows from superwinds), the large velocity widths of the Ly $\alpha$  blobs suggest that they are the sites of massive galaxy formation. If we assume gravitationally-bound gas clouds, the dynamical masses of the Ly $\alpha$  blobs are estimated to be  $\sim 10^{12} - 10^{13} M_{\odot}$ . Even for the case of outflows, the outflow velocities are likely to be the same order of the rotation velocities as inferred from the observational evidence for local starburst galaxies.

*Subject headings:* cosmology: observations — galaxies: evolution — galaxies: formation — galaxies: high-redshift — galaxies: starburst

---

<sup>1</sup>The data presented herein were obtained at the W.M. Keck Observatory, which is operated as a scientific partnership among the California Institute of Technology, the University of California and the National Aeronautics and Space Administration. The Observatory was made possible by the generous financial support of the W.M. Keck Foundation.

<sup>2</sup>Based on data collected at Subaru Telescope and in part obtained from data archive at Astronomical Data Analysis Center, which are operated by the National Astronomical Observatory of Japan.

<sup>3</sup>Department of Astronomy, Kyoto University, Sakyo-ku, Kyoto 606-8502, Japan; matsdayi@kusastro.kyoto-u.ac.jp

<sup>4</sup>National Astronomical Observatory of Japan, Mitaka, Tokyo 181-8588, Japan; yamada@optik.mtk.nao.ac.jp

<sup>5</sup>Research Center for Neutrino Science, Graduate School of Science, Tohoku University, Aramaki, Aoba, Sendai 980-8578, Japan; haya@awa.tohoku.ac.jp; yamauchi@awa.tohoku.ac.jp; y.naka@awa.tohoku.ac.jp

## 1. INTRODUCTION

Ly $\alpha$  blobs (LABs) are diffuse, large and radio-quiet Ly $\alpha$  nebulae often discovered in galaxy overdense regions at high redshifts (Keel et al. 1999; Steidel et al. 2000, hereafter S00; Francis et al. 2001; Palunas et al. 2004; Matsuda et al. 2004, hereafter M04). Recent observations revealed that a significant fraction of LABs has large luminosity of infrared dust continuum emission (Chapman et al. 2001; Smail et al. 2003; Dey et al. 2005; Geach et al. 2005; Colbert et al. 2006) and that some LABs have large ( $\gtrsim 1000 \text{ km s}^{-1}$ ) Ly $\alpha$  velocity widths (S00; Ohyama et al. 2003; Bower et al. 2004; Dey et al. 2005; Wilman et al. 2005). Although their physical origins are still unclear, three models have been proposed, (i) photo-ionization by hidden AGNs or starbursts (S00; Chapman et al. 2001; Busu-Zych & Scharf 2004; Furlanetto et al. 2005), (ii) Ly $\alpha$  cooling radiation by gravitational heating (Haiman et al. 2000; Fardal et al. 2001; Dijkstra et al. 2005), and (iii) shock heating by starburst driven galactic superwinds (Taniguchi & Shioya 2000; Ohyama et al. 2003; Mori et al. 2004).

On the other hand, a large number of compact Ly $\alpha$  emitters (LAEs) have been discovered (Cowie & Hu 1998; Fynbo et al. 2003; Ouchi et al. 2003; Shimasaku et al. 2004; Hayashino et al. 2004). Their compact morphology suggests that they are small building blocks of galaxies (Pascarelle et al. 1998). Their faint rest frame optical luminosity suggests that they are young or have small stellar masses (Yamada et al. 2001). They do not show large infrared luminosity (De Breuck et al. 2004). They show narrow (a few hundred  $\text{km s}^{-1}$ ) Ly $\alpha$  velocity widths (Hu et al. 2004; Dawson et al. 2004; Venemans et al. 2005). Giant LABs such as discovered in S00 are known to be 20 – 40 times larger than typical compact LAEs. However, M04 revealed the existence of a large number of slightly smaller and fainter blobs that show rather continuous distribution in Ly $\alpha$  spatial extents between giant LABs and compact LAEs. It is thus also important to understand the relation between LABs and compact LAEs in order to reveal the nature of LABs.

In this letter, we report the results of an intermediate resolution ( $\sim 2 \text{ \AA}$ ) spectroscopy of Ly $\alpha$  sources ranging from giant LABs to compact LAEs at  $z = 3.1$  in the SSA22 field. Matsuda et al. (2005) previously obtained 56 spectra for LAEs in the same field, but the depths and the spectral resolution were insufficient to examine their line profiles. We assume an  $\Omega_M = 0.3$ ,  $\Omega_\Lambda = 0.7$  universe with  $H_0 = 70 \text{ km s}^{-1} \text{ Mpc}^{-1}$  ( $1''$ .0 corresponds to 7.6 kpc of physical length at  $z = 3.1$ ).

## 2. OBSERVATIONS

The spectroscopic targets were chosen from candidate Ly $\alpha$  sources identified in M04. We briefly describe the selection criteria below. We used narrow-band ( $NB497$ ;  $4977\text{\AA}/77\text{\AA}$ ) and broad-band images in the SSA22 field ( $\alpha = 22^{\text{h}}17^{\text{m}}34^{\text{s}}.0$ ,  $\delta = +00^{\circ}17'01''$ , [J2000]) obtained with the Suprime-Cam (Miyazaki et al. 2002) on the 8.2 m Subaru telescope. The average stellar profile of the images has a full width at half maximum (FWHM) of  $1''.0$ . The object detection was made on a continuum subtracted narrow-band ( $NB_{\text{corr}}$ ) image smoothed with a Gaussian kernel with a FWHM of  $1''$  using a threshold of emission line surface brightness of  $2.2 \times 10^{-18} \text{ ergs s}^{-1} \text{ cm}^{-2} \text{ arcsec}^{-2}$ . The magnitudes and colors are calculated by the *same* isophotal apertures determined on the smoothed  $NB_{\text{corr}}$  image with the same isophotal limit as the detection threshold. We selected 277 candidate Ly $\alpha$  sources, which satisfy the following criteria: (1)  $NB497 < 25$  AB mag, and (2) observed equivalent width  $EW_{\text{obs}} > 80 \text{ \AA}$  (or Ly $\alpha$  luminosity  $L(\text{Ly}\alpha) > 1.7 \times 10^{42} \text{ erg s}^{-1}$  at  $z = 3.1$ ) (Fig. 1). We denote them as No. 001 through No. 277 in order of isophotal areas. The largest 35 candidates with isophotal areas  $\geq 16 \text{ arcsec}^2$  (or  $\geq 900 \text{ kpc}^2$  at  $z = 3.1$ ) are identical with the LABs presented in M04. The candidates lying near the solid curve in Figure 1 (the expected values for point sources) are not resolved in the narrow-band image. We will call the smallest 129 candidates (No. 149 – No. 277) with the isophotal areas  $< 8 \text{ arcsec}^2$ , compact LAEs.

We carried out spectroscopic observations of 37 out of the 277 candidates using the DEIMOS spectrograph (Faber et al. 2003) on the 10 m Keck II telescope in August 14–18 2004 (UT). The 37 targets are widely distributed in isophotal areas (see Fig. 1). The field of view of a slit mask is about  $5' \times 16'$ . We used the 900 l/mm grism and the GG455 filter. The typical wavelength coverage is  $\sim 4550 - 7500 \text{ \AA}$ . The slit widths for all objects are  $1''.0$ . The slit lengths range from  $6''$  to  $32''$  in order to obtain sky outside of their Ly $\alpha$  spatial extents. The spectral resolution is  $2.2 \text{ \AA}$  at  $5000 \text{ \AA}$  or a velocity resolution of  $125 \text{ km s}^{-1}$ . The pixel sampling is  $0.44 \text{ \AA}$  in wavelength and  $0''.12$  in spatial direction. We used one slit mask in this observing run. Total exposure time was 7 hours with each 30 minutes exposure. The seeing ranged from  $0''.8$  to  $1''.3$ . We reduced the data using spec2d pipeline. For analysis of integrated line profiles discussed in this letter, we made one dimensional spectra combining  $1''.1 \times 1''.0$  around emission line peaks. While extended emission lines were clearly detected for some objects, a study of the faint outskirts with lower signal-to-noise ratio (S/N) needs further careful analysis and the results will be presented elsewhere in the future. The spectra are not flux calibrated.

### 3. RESULTS

We detected emission-lines for all the observed 37 spectra with peaks above S/N of 3 per spectral resolution. The emission lines have variety in their line profiles (Fig. 2). For example, No. 004 has double peaks. The both blueshifted and redshifted emission lines have clear asymmetry. When we use statistics of line asymmetry<sup>1</sup>,  $a_\lambda$  and  $a_f$ , proposed by Rhoads et al. (2003), the lines have values of  $a_\lambda = 0.33$ ,  $a_f = 0.48$  (the blueshifted line), and  $a_\lambda = 3.6$ ,  $a_f = 4.5$  (the redshifted line). These values show that the blueshifted line has a steeper drop on the red side than the blue side, and the redshifted line has opposite asymmetry. Thus, it is reasonable to interpret them as a relatively broad emission line with a single narrow absorption. No. 031 has line profile similar to that of No. 004. Similar line profiles were also reported for LAB2 in the same field (Wilman et al. 2005),  $z \sim 3.1$  LAEs around a radio galaxy (Venemans et al. 2005) and radio galaxies at  $z \sim 2.5 - 4$  (Wilman et al. 2004). No. 030 has a single peaked emission line with a strong absorption on the blue side ( $a_\lambda = 2.2$ ,  $a_f = 1.9$ ). No. 103, 151 and 241 have symmetric single narrow emission lines ( $a_\lambda = 0.7 - 1.3$ ,  $a_f = 0.7 - 1.0$ ). Although these lines do not show clear asymmetry often seen in Ly $\alpha$  emission lines at higher redshifts (e.g. Hu et al. 2004; Dawson et al. 2004), this may be due to the fact that the effect of absorptions by intergalactic H I clouds on the blue side of Ly $\alpha$  line is weaker at  $z \sim 3$  (Songaila et al. 2004). These spectra show no other emission lines to suggest that the identified lines are not Ly $\alpha$ . The spectral resolution of 2.2 Å is sufficient to resolve foreground [O II] $\lambda\lambda$ 3726, 3729 doublets if there are. Only one object (No. 237) turns out to be a  $z = 0.33$  [O II] emitter, as it has very narrow double peaked emission lines with the separation of  $\sim 4$  Å, and [O III] $\lambda\lambda$ 4959, 5007 and H $\beta$  at longer wavelength (Fig. 3). No. 053 and 070 have the broadest emission lines and show C IV emission lines at longer wavelength. Their broad Ly $\alpha$  emission lines are likely to be due to AGNs in the objects.

We examined the *entire* velocity widths of the Ly $\alpha$  emission lines by fitting a single Gaussian function. We used only emission line part (i.e. within  $\sim \pm 4$  times the dispersion of the Gaussian function), and masked possible absorption lines as shown in Figure 2. If the spectra show double peaks, we masked the region between the peaks. We then studied the distribution of Ly $\alpha$  velocity widths of 28 objects with peaks above S/N of 6 per spectral resolution without 2 AGNs. They have the velocity widths (FWHM) in the range of 150 – 1700 km s<sup>-1</sup>, with a median of 550 km s<sup>-1</sup>. The widths are corrected for the instrumental

---

<sup>1</sup>The “wavelength ratio” is defined as  $a_\lambda = (\lambda_{10,r} - \lambda_p)/(\lambda_p - \lambda_{10,b})$  and the “flux ratio” as  $a_f = \int_{\lambda_p}^{\lambda_{10,r}} d\lambda / \int_{\lambda_{10,b}}^{\lambda_p} d\lambda$ , where  $\lambda_p$  is the wavelength of the peak of the emission line, and  $\lambda_{10,b}$  and  $\lambda_{10,r}$  are the points at which the line flux exceeds 10% of the peak on the blue side and the red side respectively.

resolution. The 12 LABs have the widths of  $\gtrsim 500 \text{ km s}^{-1}$ , with a median of  $780 \text{ km s}^{-1}$ . The 7 compact LAEs have the widths of  $\lesssim 700 \text{ km s}^{-1}$ , with a median of  $280 \text{ km s}^{-1}$ . Venemans et al. (2005) reported that  $z \sim 3.1$  LAEs around a radio galaxy have the widths in the range of  $120 - 800 \text{ km s}^{-1}$ , with a median of  $260 \text{ km s}^{-1}$ . These values are very similar to those of our compact LAEs. We plot the Ly $\alpha$  velocity widths and the Ly $\alpha$  isophotal areas in Figure 4. There is a correlation between the velocity widths and the isophotal areas. A Spearman rank correlation analysis shows that the correlation has  $r_s = 0.59$  and significance level of 99.9%. The uncertainties of velocity widths by the fit are shown in Figure 4. We also estimated the uncertainties of the isophotal areas as follows. We put  $40'' \times 40''$   $NB_{\text{corr}}$  images of each object at 100 random positions on the original  $NB_{\text{corr}}$  image and re-measured the isophotal areas. Note that the derived uncertainties of the isophotal areas may be slightly overestimated because the re-measured isophotal areas were affected by combinations of noise from the thumbnail images of the objects and the original  $NB_{\text{corr}}$  image.

#### 4. DISCUSSION

We found the correlation between the Ly $\alpha$  velocity widths and the Ly $\alpha$  isophotal areas and that all the LABs have the widths of  $\gtrsim 500 \text{ km s}^{-1}$ . There are several possible physical interpretations of the Ly $\alpha$  velocity widths; motion of gravitationally-bound gas clouds, inflows, merging of clumps, or outflows from superwinds.

We consider the first case that the Ly $\alpha$  velocity widths are due to motion of gravitationally-bound gas clouds within collapsed dark matter halos. If we assume random motions in a singular isothermal sphere ( $\rho \propto r^{-2}$ ), the dynamical mass can be estimated to be  $M_{\text{dyn}} = 3\sigma^2 r/G$ , or

$$M_{\text{dyn}} = 5.2 \times 10^{12} M_{\odot} \left( \frac{\sigma}{500 \text{ km s}^{-1}} \right)^2 \frac{r}{30 \text{ kpc}} \quad (1)$$

where  $\sigma$  is one dimensional velocity dispersion,  $G$  is the gravitational constant and  $r$  is the radius of Ly $\alpha$  nebulae. When we use the radius of a circle with area which is equivalent to the Ly $\alpha$  isophotal area, the dynamical masses of the 12 LABs are estimated to be  $5 \times 10^{11} - 2 \times 10^{13} M_{\odot}$  (Fig. 4a). The mass estimation suggests that LABs already have their massive halos comparable to those of present day massive galaxies. If we consider inflows or merging of clumps, the gas clouds or clumps may have not yet been accelerated enough in the gravitational potential of dark matter halos. In these cases, the mass estimation may give lower limits.

We consider the next case that the Ly $\alpha$  velocity widths are due to gas outflows from superwinds. In this case, the velocity widths may not represent the masses of the objects.

Heckman et al. (2000) reported that there is no tight correlation between the rotation velocities and the outflow velocities for low redshift starburst galaxies. Martin (2005), however, recently revisited the issue and revealed a correlation with a larger sample. If the same correlation holds at high redshifts, Ly $\alpha$  sources with larger velocity widths would have larger dynamical masses. If we assume outflows from a central starburst, we can also estimate the characteristic time-scales of star-formation by their spatial extents and typical outflow speeds. If we divide  $2r$  by the Ly $\alpha$  velocity widths, the time-scales are estimated to be in the range of  $3 \times 10^7 - 10^8$  yr (Fig. 4b). Note that the time-scales are only upper limits for unresolved compact LAEs. Geach et al. (2005) suggested that the LABs have average star-formation rate of  $\sim 10^3 M_{\odot} \text{ yr}^{-1}$  by their sub-mm observations. If the LABs have continuous star formation at this rate for several  $\times 10^7$  yr, they would have large stellar masses of several  $\times 10^{10} M_{\odot}$ .

Thus the large velocity widths of LABs imply that they are indeed hosted in the massive systems. Their large spatial extents, large Ly $\alpha$  luminosity, and rather chaotic structures seen in their line profiles, as well as high sub-mm detection rate, also support that they are in active forming phase.

We thank the anonymous referee for useful comments which have significantly improved the paper. We thank the staff of the Subaru Telescope and the Keck Telescope for their assistance with our observations. We thank K. Ohta, T. Totani, and M. Mori for useful discussions. This work is supported by the Grant-in-Aid for the 21st Century COE "Center for Diversity and Universality in Physics" from the Ministry of Education, Culture, Sports, Science and Technology (MEXT) of Japan. The research of T.Y. is partially supported by the Grant-in-Aid for scientific research from the MEXT (14540234 and 17540224). The analysis pipeline used to reduce the DEIMOS data was developed at UC Berkeley with support from NSF grant AST-0071048.

## REFERENCES

- Bower, R. G., et al. 2004, MNRAS, 351, 63
- Basu-Zych, A., & Scharf, C. 2004, ApJ, 615, L85
- Chapman, S. C., Lewis, G. F., Scott, D., Richards, E., Borys, C., Steidel, C. C., Adelberger, K. L., & Shapley, A. E. 2001, ApJ, 548, L17
- Colbert, J. W., Teplitz, H., Francis, P., Palunas, P., Williger, G. M., & Woodgate, B. 2006, ApJ, 637, L89
- Cowie, L. L., & Hu, E. M. 1998, AJ, 115, 1319
- Dawson, S., et al. 2004, ApJ, 617, 707
- De Breuck, C., et al. 2004, A&A, 424, 1
- Dey, A., et al. 2005, ApJ, 629, 654
- Dijkstra, M., Haiman, Z., & Spaans, M. 2005b, ArXiv Astrophysics e-prints, arXiv:astro-ph/0510409
- Faber, S. M., et al. 2003, Proc. SPIE, 4841, 1657
- Fardal, M. A., Katz, N., Gardner, J. P., Hernquist, L., Weinberg, D. H., & Davé, R. 2001, ApJ, 562, 605
- Francis, P. J., et al. 2001, ApJ, 554, 1001
- Furlanetto, S. R., Schaye, J., Springel, V., & Hernquist, L. 2005, ApJ, 622, 7
- Fynbo, J. P. U., Ledoux, C., Möller, P., Thomsen, B., & Burud, I. 2003, A&A, 407, 147
- Geach, J. E., et al. 2005, MNRAS, 363, 1398
- Haiman, Z., Spaans, M., & Quataert, E. 2000, ApJ, 537, L5
- Hayashino, T., et al. 2004, AJ, 128, 2073
- Heckman, T. M., Lehnert, M. D., Strickland, D. K., & Armus, L. 2000, ApJS, 129, 493
- Hu, E. M., Cowie, L. L., Capak, P., McMahon, R. G., Hayashino, T., & Komiyama, Y. 2004, AJ, 127, 563
- Keel, W. C., Cohen, S. H., Windhorst, R. A., & Waddington, I. 1999, AJ, 118, 2547

- Martin, C. L. 2005, ApJ, 621, 227
- Matsuda, Y., et al. 2004, AJ, 128, 569
- Matsuda, Y., et al. 2005, ApJ, 634, L125
- Miyazaki, S., et al. 2002, PASJ, 54, 833
- Mori, M., Umemura, M., & Ferrara, A. 2004, ApJ, 613, L97
- Ohyama, Y., et al. 2003, ApJ, 591, L9
- Ouchi, M., et al. 2003, ApJ, 582, 60
- Palunas, P., Teplitz, H. I., Francis, P. J., Williger, G. M., & Woodgate, B. E. 2004, ApJ, 602, 545
- Pascarelle, S. M., Windhorst, R. A., & Keel, W. C. 1998, AJ, 116, 2659
- Rhoads, J. E., et al. 2003, AJ, 125, 1006
- Shimasaku, K., et al. 2004, ApJ, 605, L93
- Smail, I., Ivison, R. J., Gilbank, D. G., Dunlop, J. S., Keel, W. C., Motohara, K., & Stevens, J. A. 2003, ApJ, 583, 551
- Songaila, A. 2004, AJ, 127, 2598
- Steidel, C. C., Adelberger, K. L., Shapley, A. E., Pettini, M., Dickinson, M., & Giavalisco, M. 2000, ApJ, 532, 170
- Taniguchi, Y., & Shioya, Y. 2000, ApJ, 532, L13
- Venemans, B. P., et al. 2005, A&A, 431, 793
- Wilman, R. J., Jarvis, M. J., Röttgering, H. J. A., & Binette, L. 2004, MNRAS, 351, 1109
- Wilman, R. J., Gerssen, J., Bower, R. G., Morris, S. L., Bacon, R., de Zeeuw, P. T., & Davies, R. L. 2005, Nature, 436, 227
- Yamada, T., et al. 2001, PASJ, 53, 1119



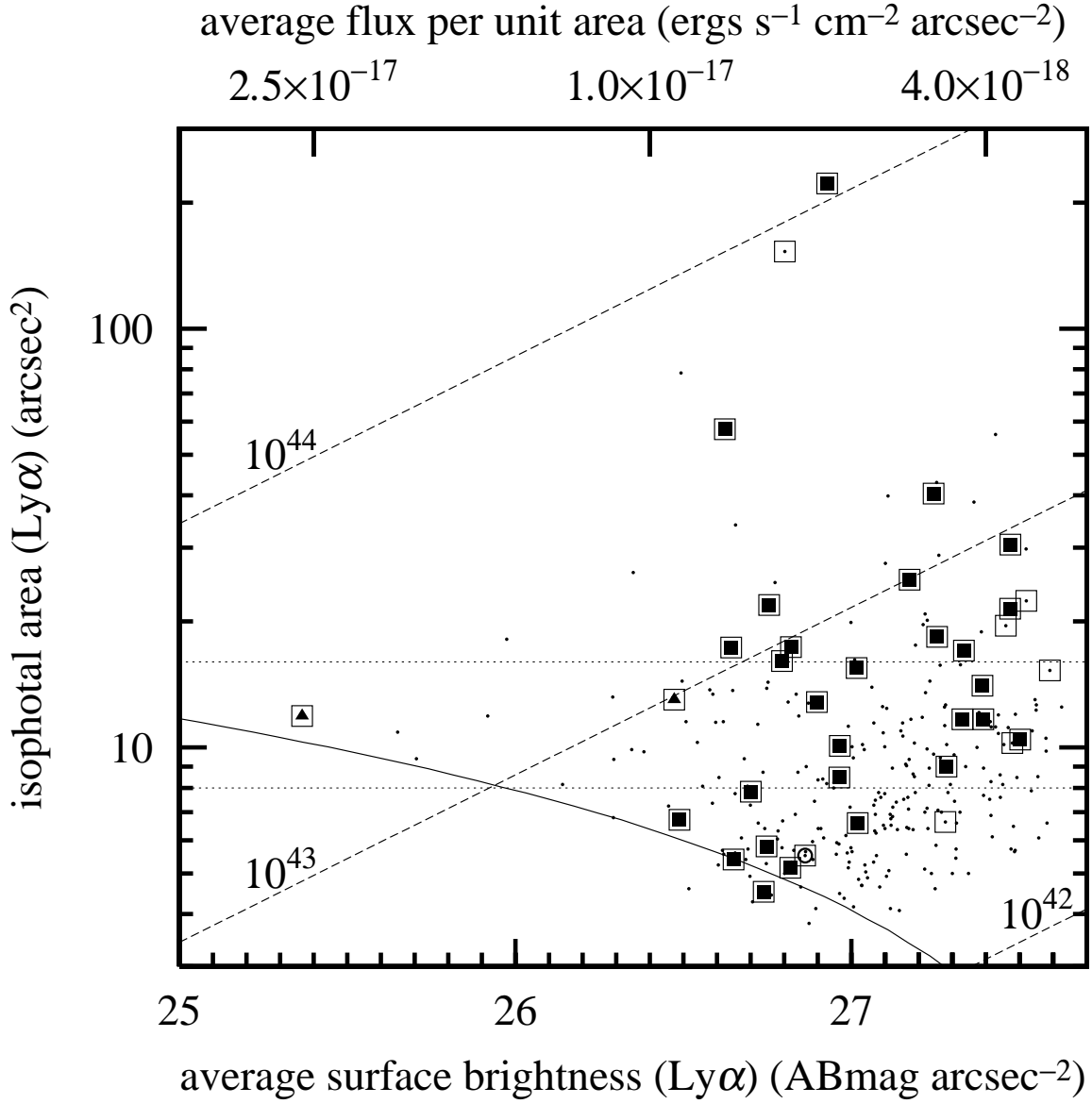


Fig. 1.— Distribution of Ly $\alpha$  isophotal area and Ly $\alpha$  average surface brightness for candidate Ly $\alpha$  sources. The dots show the 277 candidates. The large open squares show the 37 spectroscopic targets. The filled squares show the 28 Ly $\alpha$  sources which show Ly $\alpha$  emission lines with S/N>6 per spectral resolution of 2.2 Å. The filled triangles show AGNs at  $z = 3.1$ . The open circle shows a [O II] emitter at  $z = 0.33$ . The long dashed lines correspond to the Ly $\alpha$  luminosity of  $10^{44}$ ,  $10^{43}$  and  $10^{42}$  ergs s $^{-1}$ . The short dashed horizontal lines show the sample thresholds of the isophotal areas of 16 arcsec $^2$  for LABs and 8 arcsec $^2$  for compact LAEs.

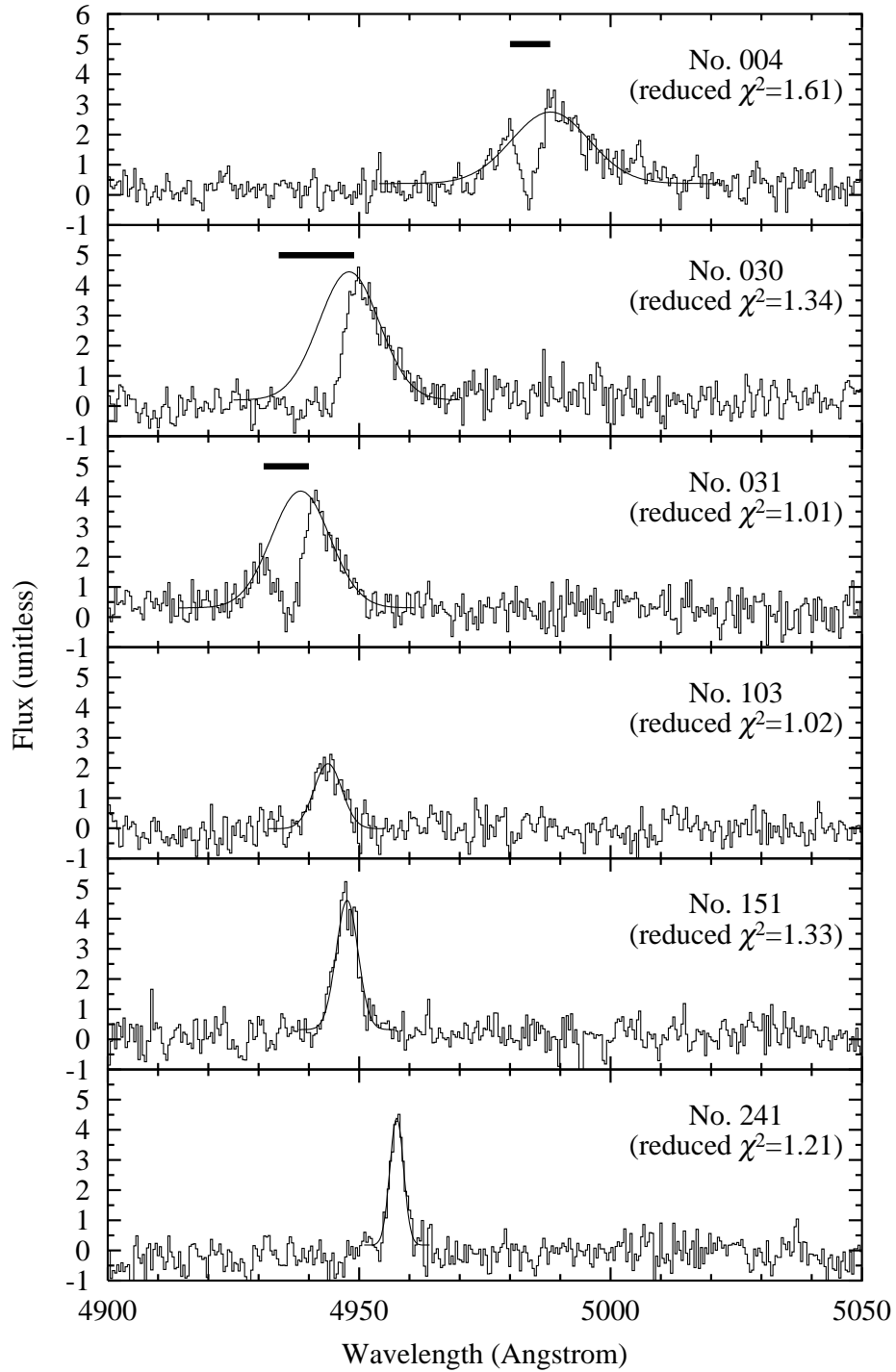


Fig. 2.— Examples of 1 dimensional spectra of Ly $\alpha$  sources. The solid curves show the best fit Gaussian profiles. The thick bars show masked regions.

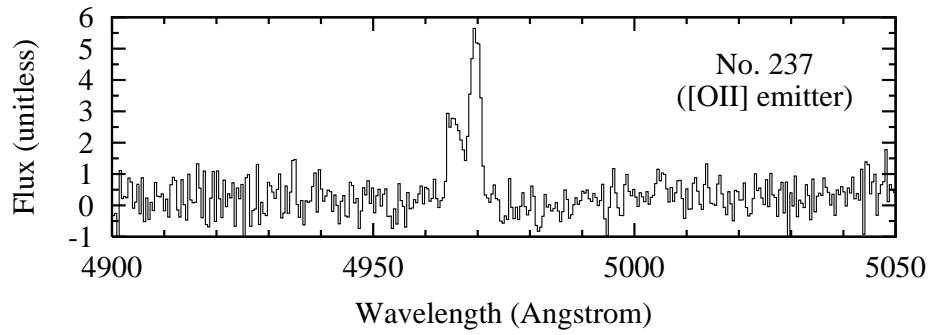


Fig. 3.— A spectrum of a foreground [O II] emitter at  $z = 0.33$  in the spectroscopic sample. The spectral resolution of  $2.2 \text{ \AA}$  is sufficient to resolve [O II] $\lambda\lambda 3726, 3729$  doublets.

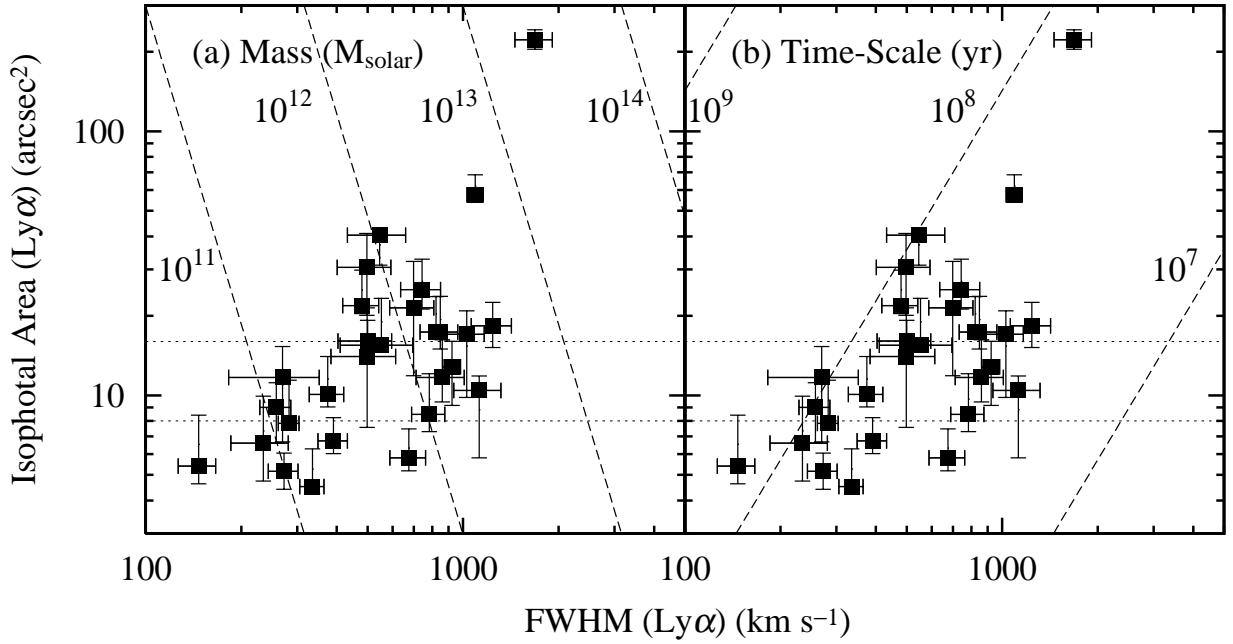


Fig. 4.— Distribution of  $\text{Ly}\alpha$  isophotal area and  $\text{Ly}\alpha$  velocity width (FWHM). The filled squares show 28  $\text{Ly}\alpha$  sources with the  $\text{Ly}\alpha$  emission line peaks above S/N of 6 per spectral resolution of  $2.2 \text{ \AA}$ . The short dashed horizontal lines show the sample thresholds of the isophotal areas of  $16 \text{ arcsec}^2$  for LABs and  $8 \text{ arcsec}^2$  for compact LAEs. (*left panel*) The long dashed lines show the estimated dynamical masses of  $10^{11}$ ,  $10^{12}$ ,  $10^{13}$ ,  $10^{14} M_{\odot}$  assuming motion of gravitationally-bound gas clouds. (*right panel*) The dashed lines show the estimated time-scales of star-formation of  $10^7$ ,  $10^8$ ,  $10^9 \text{ yr}$  assuming outflows from superwinds.